Do mechanical strain magnitude and rate drive bone adaptation in adult women? A 12-month prospective study.

Karen L. Troy[1], Megan E. Mancuso[1], Joshua E. Johnson[1], Zheyang Wu[2], Thomas J. Schnitzer[3], Tiffiny A. Butler[1]

June 29, 2018

[1] Department of Biomedical Engineering, Worcester Polytechnic Institute, Worcester, MA

[2] Department of Mathematical Sciences, Worcester Polytechnic Institute, Worcester, MA

[3] Department of Physical Medicine and Rehabilitation, Northwestern University, Chicago, IL

Corresponding Author:

Karen L. Troy, PhD

Associate Professor, Biomedical Engineering

Worcester Polytechnic Institute

100 Institute Road

Worcester, MA 01609

Email: ktroy@wpi.edu

Tel. 508-831-6093

Abstract

Although there is strong evidence that certain activities can increase bone density and structure in some individuals, it is not clear what specific mechanical factors govern the response. Animal *in vivo* loading models have demonstrated that mechanical signals related to strain rate and strain magnitude regulate bone adaptation. However, the degree to which these parameters govern bone adaptation in humans has never been prospectively tested. Here, we quantified the degree to which bone strain influences bone adaptation in the upper extremity of healthy adult women during a twelve month prospective study period. One hundred and two women age 21-40 participated in one of two experiments. Experiment 1: low (n=21) and high (n=24) strain magnitude. Experiment 2: low (n=21) and high (n=20) strain rate. Control group (n=16): no intervention. Strains were assigned using CT-derived subject-specific finite element (FE) models. Load cycles were recorded digitally, and analyzed for magnitude and rate characteristics. The primary outcome was change in ultradistal integral bone mineral content (iBMC), assessed with quantitative CT. Interim timepoints and secondary outcomes were assessed with high resolution peripheral quantitative CT (HRpQCT). Sixty subjects completed all 12-months of the intervention, and interim timepoint data were analyzed for 77 subjects. Both the low and high strain rate groups had significant 12-month increases to ultradistal iBMC (percent change in control: -1.3±2.7%, low strain rate: 2.9±2.0%, high strain rate: 3.6±2.3%), total iBMC, and other measures. A “loading dose” measure consisting of Strain_MagRate = mean(Peak-to-Peak Strain Magnitude)*mean(Strain Rate)*(#bouts) was significantly and positively related to 12-month change ultradistal integral BMC, and 3 or 9-month changes to total BMD, cortical thickness and inner trabecular BMD. Subjects who gained the most bone had, on average, completed 130 loading bouts of (mean strain) 550 με at 1805 με/s, over a period of 12 months. Those with the greatest gains had the highest Strain_MagRate loading dose. We conclude that signals related to strain magnitude, strain rate, and number of loading bouts collectively contribute to bone adaptation in healthy adult women.

Introduction

Exercise-based interventions have long been considered a viable option for preserving and enhancing bone strength [1] because bone adapts to best resist its habitual mechanical loading environment. Individuals who play sports and load with odd strains (soccer, squash) have been observed to have better bone mechanical properties than those who do not [2]. Furthermore, clinical trials have shown that high impact activities such as jumping and hopping can improve bone density in growing children [3] and young adults [4] and maintain bone density in older adults [5]. However, while the evidence is strong that certain activities can increase bone density and structure in some individuals, it is not clear what specific mechanical factors govern the response. Furthermore, these factors interact with each individual person's physiology to create a variable response, which is not well understood.

Animal *in vivo* loading models have demonstrated that mechanical signals related to strain rate [6-8] and strain magnitude [9; 10] regulate bone adaptation. There is no consensus on which specific signal(s) osteocytes sense; evidence supports lacunar-cannilicular fluid flow [11; 12], flow of ions and the resulting electromagnetic signal [13], direct damage of osteocytes [14], microdamage of the surrounding bone that results in altered stress or strain [15; 16] and other candidates [17]. Regardless of the exact mechanism, all of these signals are closely related to (and driven by) mechanical strain. *In vivo* loading models have also established that, to elicit an adaptive response, the mechanical signal must be both dynamic and novel [18]. Despite extensive animal literature, the degree to which mechanical strain magnitude and rate govern bone adaptation in humans has never been prospectively tested.

One major challenge is that bone strain is difficult to measure noninvasively. As a result, indirect measures, such as surveys for physical activity, which include weighting factors based on experimentally measured ground reaction force (GRF) and rate of GRF have been proposed [19; 20]. Others have proposed "bone loading" indices that are based on similar measures (e.g. accelerometry) [21; 22]. While these can be helpful in identifying the types of activities that should theoretically elicit an osteogenic response, they do not account for individual differences in bone

structure, which have a large influence on bone strain [23]. Validated subject-specific FE models can estimate bone strain *in vivo* during specific tasks, and can provide insight into the problem. While FE models can provide accurate estimates of bone strain [24-26], they require detailed knowledge of the specific boundary conditions (magnitude, direction, and locations of application) of the mechanical loads that are transmitted through the bone.

Our previously validated upper extremity loading model [26] provides a well-controlled framework to understand the degree to which strain magnitude and rate influence bone adaptation in people. In this model, an individual produces a compressive force through the radius by leaning onto the palm of the hand to achieve a target force. Feedback is given using a scale or loadcell, and individuals are given sound cues to assist in achieving a regular and consistent load/unload cycle. In a pilot group of 19 young adult women, we found that a mean energy equivalent strain of 734 ± 238 με applied 50 cycles per day, 3 days per week elicited modest increases in distal radius bone mineral content (BMC) and prevented seasonal loss of BMC observed in a control group [26]. We also observed that high strain regions of the radius gained significantly more bone than low strain regions, suggesting that the local mechanical signals were, in part, driving the response [27]. Although these results were promising, the study was limited in scope and duration.

Here, our purpose is to quantify the degree to which bone strain influences bone adaptation in the upper extremity of healthy adult women during a twelve month prospective study period. We hypothesize that (1) bone accrual is proportional to strain magnitude and strain rate, and (2) structural changes include increased cortical diameter and thickness, and increased trabecular bone mass near the endosteal surface.

Methods

Participant Characteristics

One hundred and two women, age: 28 ± 6 years, height: 164 ± 8 cm, mass: 65 ± 9 kg, were recruited from the community for this randomized controlled trial. Healthy women age 21-40 were included in the present study; this group is at peak bone mass [28; 29], and compared to

men, have increased risk of osteoporosis later in life. After initial telephone screening for inclusion criteria, potential subjects were screened with dual energy x-ray absorptiometry (DXA) of the non-dominant radius and circulating levels of 25-hydroxyvitamin vitamin D and estradiol. Exclusion criteria included BMI outside [18-25 kg/m^2], irregular menstrual cycles, no regular calcium intake, use of medications affecting bone health, history of radius fracture or injury to the non-dominant shoulder or elbow, regular participation (>2 times per month) in activities with high loads at the forearm (e.g. gymnastics, volleyball), 25-hydroxyvitamin D serum levels below 20 ng/ml, and DXA T-score outside [-2.5 to 1.0]. In total, 102 potential participants provided written, informed consent prior to participation in this institutionally approved study. All subjects were recruited at a single site between December 2013 and June 2017. The trial was conducted in accordance with Good Clinical Practice Guidelines. Compliance and adverse events data were reviewed annually with a study monitor.

Study Design

The study consisted of a 12 month, prospective, randomized trial with a distal radius compressive loading intervention. After obtaining informed consent,subjects were randomized into either control or one of two exercise arms that manipulated strain magnitude (Experiment 1: low and high strain magnitude) or strain rate (Experiment 2: low and high strain rate, detailed in Table 1). Exercise groups were instructed to apply 100 cycles of axial force (one bout), four times weekly, by leaning onto the palm of the hand. Loading was accomplished using a custom device, consisting of a uniaxial load cell (Standard Load Cells; Gujarat, India), data logger (DATAQ DI-710), and LED indicators that lit up when the applied force was within ±10 N of the target value. To allow subjects to get used to the intervention, those in the exercise groups were assigned a nominal 200 N target force magnitude for the first three months of loading. Thereafter, a subject-specific target force was prescribed to achieve target strain parameters using computed-tomography based finite element (FE) models (described below; Figure 1).

Due to considerations of subject safety, no subject was assigned a force larger than 450 N or what she could comfortably and consistently apply, even if the force required to achieve the

target strain was larger than that. Partway through the study, in response to reports of wrist soreness from some subjects, this upper limit was reduced to 350 N. Loading rate and cycle period were controlled using verbal instructions (e.g. “load slowly and evenly” versus “load as rapidly as possible”) and sound cues recorded on a portable voice recorder. Sound cues consisted of 100 beeps (long beeps for the slow rate group, short beeps for the fast rate group) occurring at 2-second intervals. Compliance was monitored every three months using data logger recordings and log books maintained by subjects.

The primary outcome variable was 12 month change in integral ultradistal radius bone mineral content and bone mineral density (iBMC and iBMD), as measured by quantitative CT analysis (QCT). Secondary outcomes included 12 month changes in other regions, and specific structural measures and interim timepoints. A power analysis based on pilot data [26] determined that 20 subjects per group would have 80% power to detect a 12 month change in BMC of 1.0±1.1%.

Data Collection

Demographic information and imaging data (DXA, computed tomography; CT, and high resolution peripheral computed tomography; HRpQCT) were collected at baseline. Hand dominance was determined using the Edinburgh inventory [30] and expressed as left or right decile. HRpQCT was updated every three months during the study period. CT was collected at baseline and 12 months.

High Resolution Peripheral Quantitative Computed Tomography

Changes in radius microstructure were assessed using HRpQCT (Xtreme CT I, Scanco Medical; Brüttisellen, Switzerland). Bilateral scans were acquired in a standard 9.02 mm region consisting of 110 transverse slices (82 µm isotropic voxel size) beginning 9.5 mm proximal to the distal endplate. Structural changes were measured for the mutually overlapping region. Total mean cross-sectional area (CSA; mm^2) and total volumetric bone mineral density (Tt.BMD; $mgHA/cm^3$) were measured. Trabecular number (Tb.N; mm^{-1}), thickness (Tb.Th; mm) and BMD (Tb.BMD; $mgHA/cm^3$) were measured using the manufacturer’s standard analysis

protocol. The trabecular region was further divided into inner (central 60%; Tb.BMDinn) and outer regions (outer 40%; Tb.BMDmeta). The coefficient of variation (CV) for densitometric variables is < 0.3%. Cortical vBMD (Ct.BMD; mgHA/cm^3), cortical thickness (Ct.Th; mm), and cortical porosity (Ct.Po; %) were calculated using the dual-threshold method [31-33]. The CVs of these variables range from 0.4-13%. All HRpQCT analyses were blinded to group assignment.

Quantitative Computed Tomography Analysis

At baseline and 12 months, CT scans of the distal-most 12 cm of the each forearm were acquired (GE Brightspeed, GE Medical, Milwaukee, WI, 120 kV, 180 mA, voxel size 234 µm x 234 µm x 625 µm). A calibration phantom (QRM, Moehrendorf, Germany) with known calcium hydroxyapatite equivalent concentrations was included in the field of view to relate CT attenuation (Houndsfield Units) to equivalent bone density (g/cm^3).

Changes in bone macrostructure were quantified from CT data using Mimics v15.1 (Materialise, Leuven, Belgium). Follow-up scans were registered to baseline using rigid image registration and the periosteal surface was defined using a 0.175 g/cm^3 density threshold [26]. Based on methods previously established [34], we defined integral, cortical, and endocortical compartments (denoted in QCT variable names with prefixes *i* and *ec*). Briefly, the integral compartment consisted of all voxels within the periosteal surface. The endocortical compartment was comprised of the entire set voxels located within 2.5 mm of the periosteal surface (including all cortical bone). For each compartment bone volume (BV; cm^3), bone mineral content (BMC; g) and bone mineral density (BMD; g/cm^3) were calculated. QCT parameters for the trabecular compartment were not analyzed. Instead, HRpQCT data were analyzed, which provided a greater level of detail. Using previously established methods [26], we also calculated compressive strength index (CSI; g^2/cm^4), bending strength index (BSI, cm^3), and mass-weighted principal moments of inertia (I_{min}, I_{max}, J_o, g*mm^2). All parameters were calculated for total and ultradistal regions except for strength measures, which were only calculated for the ultradistal region. The total region extended 45 mm proximal from the subchondral plate and distally to the styloid tip; the ultradistal region extended 9.375 mm proximal from the subchondral plate. The coefficient of

variation for these QCT measures in our lab ranges from 0.7 to 2.3% (ultradistal region); 0.3 to 0.6% (total region); 0.9 to 2.3% (strength indices). All QCT analyses were blinded.

Continuum Finite Element Modeling

Finite element models were constructed from the QCT scans using methods validated using cadaveric mechanical testing [35]. Models were used to simulate one cycle of axial loading to determine the subject-specific force needed to achieve the desired target strain within the distal radius. As with our previous work, we used energy-equivalent strain as the measure of interest, since it provides a scalar value that has been related to bone adaptation [27; 36]. Strain values were assigned to each subject based on the maximum energy-equivalent strain within the ultra-distal region of the radius, as calculated using the continuum FE model for that subject. The baseline FE model for each subject was used to adjust the custom loading device so that the LEDs would light up when that individual achieved her target strain. At all subsequent time points, data recorded from the load cell were applied to the FE model to calculate the *actual* mean strain within the region achieved by the subject, based on applied force (Figure 1c).

Load Cell Analysis

At each follow-up visit, load cell recordings were analyzed. The beginning, peak and end of each loading waveform were identified using a custom algorithm, and the resulting frequency spectrum calculated using a Fast Fourier Transform. Based on subject-specific FE models, frequency data were used to calculate the loading stimulus using the relationship suggested by Turner [18].

$$E = \sum_{i=0\,Hz}^{5\,Hz} \varepsilon_i f_i$$

Where E is the strain stimulus for the entire loading session, f_i is the frequency value for bin i, and ε_i is the peak-to-peak strain magnitude of frequency component i. A cutoff of 5 Hz was selected, based on analysis of the load cell frequency content, which showed that over 95% of the signal power was <2 Hz. We also calculated peak-to-peak strain magnitude and strain rate for the loading portion of each cycle for each subject and each loading bout. Because voluntary loading produced variable and sometimes inconsistent loading signals, we evaluated several

candidate measures of “loading dose”, which was intended to serve as an overall metric of mechanical loading dose, considering strain parameters and protocol compliance. We considered the following candidate measures of “loading dose”.

StrainStim = *E**[#bouts]

Strain_Mag = mean(Peak-to-Peak Strain Magnitude)*[#bouts]

Strain_Rate = mean(Strain Rate)*[#bouts]

Strain_MagRate = mean(Peak-to-Peak Strain Magnitude)*mean(Strain Rate)*[#bouts]

Statistical Analysis

Descriptive statistics were calculated and assessed for normality. Group demographics and loading dose received were compared using ANOVA, with Boneferroni-corrected *post hoc* t-tests. Analyses were initially by intention to treat. The hypothesis that bone mass would increase proportionally to applied strain magnitude (Experiment 1) was tested in two ways. First, subjects were analyzed by group (control vs. low and high strain magnitude groups). For the group analysis, the 12-month change in ultradistal iBMC was analyzed as the primary dependent variable in a linear regression model with coefficients representing contrasts between each of the two experimental groups and the control group. Secondary outcome measures were also compared between groups using regression models for change scores at each of the time points (change from baseline). Similar analyses were performed to examine the effect of strain rate on bone (Experiment 2).

In the second analysis, we considered “loading dose” achieved by each subject as a continuous variable, with the dose for control subjects being zero. Because dose includes both magnitude and frequency components, all groups were combined into a single regression model with 12 month change in radius ultradistal iBMC as the primary outcome. Secondary outcome measures were also considered. To test the hypothesis that bone structural changes would include increased cortical diameter and thickness, and increased endocortical density, these parameters were treated as dependent variables in linear regression models, similar to the previous analyses. We assessed the F-statistic of the overall regression, and the t-statistic of each explanatory

variable, considering α=0.05 to be significant. As an exploratory *post hoc* analysis, subjects were grouped into tertile, based on the change in ultradistal iBMC. Subject demographics, baseline values, and loading dose were compared between tertiles, to gain insight into what factors were associated with the most gains in ultradistal iBMC. Bonferroni-adjusted *post hoc* t-tests were used to compare individual tertiles.

Results

Participant Characteristics

Baseline characteristics are summarized in Table 1 and were not different between experimental groups. Sixty subjects completed the study and were included in the 12-month analysis. Seventy-seven subjects had some follow-up data available and were included in our analyses of interim time points (Figure 2). On average, subjects assigned to one of the loading groups completed 85 ± 85 loading bouts in total. However, the total number of loading bouts varied considerably, from 0 to 357. All measures of loading dose were significantly greater for loading groups than for controls ($p<=0.046$; Table 1)

Adverse Events

There were no serious adverse events. Temporary soreness of the loaded wrist was the most commonly reported adverse event (28% of subjects; 29 reports). Two of these subjects noted that this briefly affected their daily activities (did fewer chores or avoided exercises that weighted the hands), and one took ibuprofen. Eight subjects reported soreness at other sites (elbow, shoulder, hand), which included aggravation of previous injuries (e.g. shoulder pain from an injury that was several years old) that they thought might be due to the loading intervention. All subjects reported that soreness resolved within 3-14 days. Five subjects reported that pain from previous injuries temporarily prevented them from completing the assigned loading, but did not believe this was caused or aggravated by the intervention. Radiology reports indicated no visible changes in wrist anatomy between initial and 12 month visits. Lack of time or relocation were the most common reasons expressed for dropping out (22 subjects).

Effect of Strain on 12-month Change in Bone Mass and Structure (QCT)

None of the regression models that included strain magnitude groups were significant for overall model fit, although the membership in the low strain magnitude group was associated with slight gains in ultradistal iBMC (p=0.041). Individuals in the low magnitude loading group experienced a 4.9 ± 14.6 mg increase to ultradistal iBMC, compared to a 10.6 ± 24.1 mg decrease in the control group (Table 2).

Strain rate had a stronger effect on 12 month change in QCT variables than did strain magnitude. In models comparing the low and high strain rate groups to the control group, both loading groups were significantly and positively associated with increases to total and ultradistal iBMC and iBMD. The low strain rate group also had significant increases in ecBMC. Over 50% of the variance in change to ultradistal and total iBMD was explained by group membership for these subjects. Increases to ultradistal compressive and bending strength indices were significantly and positively associated with Experiment 2 loading group membership (Table 2).

In models examining the effect of loading dose on changes to bone, ultradistal iBMC, iBV, and endocortical BV were all positively and consistently associated with measures of loading dose, especially Strain_MagRate (Figure 2). However, in all cases, loading dose explained less than 15% of the variance in the change values.

Effect of Strain on 3, 6, 9, and 12 Month Bone Microstructure (HRpQCT)

After three months, membership in the low and high magnitude loading groups explained up to 17% of the increases in Tt.BMD compared to the control group (Table 3). Similarly, high loading rate was associated with significant three-month increases to Tt.BMD, Ct.BMD and Ct.Th (Table 3). Strain_MagRate, Strain_Mag, and Strain_Rate were all significant predictors of change in Tt.BMD and Ct.Th, although 12% or less of the variance in these measures was explained by loading dose.

At six months, none of the microstructural changes were different between groups. However, at nine months, the low strain magnitude group was significantly and positively associated with increases to Tt.BMD, Tb.BMD, Tb.BMDinn, and Tb.BMDmeta (Figure 3).

Similarly, the high strain magnitude and low strain rate groups were positively associated with changes to Tb.BMDinn. Strain_MagRate and Strain_Rate were also positively associated with increases to Tb.BMDinn at nine months (Figure 3). These changes persisted at 12 months, with Strain_MagRate being associated with increases to Tb.BMD and Tb.BMDinn.

Comparison between change in ultradistal iBMC tertile groups

Subjects in the first tertile gained bone, the middle tertile had no change, and the lowest tertile lost bone. Subject age, height, weight, aBMD, and vitamin D levels were not different between tertile groups (Table 5). Those in the first tertile had higher baseline ultradistal iBMC and iBMD than the lowest tertile, but no other baseline measures differed between groups. Strain_MagRate, Strain_Mag, and Strain_Rate were all significantly different across the three tertiles, with the first tertile having the highest dose by all three measures. However, after Bonferroni adjustment for multiple comparisons, only Strain_MagRate was significantly different between the first and third tertiles.

Discussion

We conducted a randomized prospective experiment to characterize the relationship between mechanical strain magnitude and rate and changes to bone in healthy adult women. We found that the application of mechanical strain produced small but significant changes to the ultradistal radius after one year. Our first hypothesis was partially supported by the results. Membership in both the low and high strain rate groups were strongly associated with increases to total and ultradistal iBMC, iBMD, ecBMC and ecBMD. Both low and high strain rates were also associated with increases to compressive and bending strength indices. When loading dose, which included a combination of strain magnitude, strain rate, and number of loading bouts was taken into account, we observed a dose-dependent relationship between iBMC and CSA across all subjects.

Our hypothesis that structural changes would include increased cortical diameter and thickness, and increased trabecular bone mass near the endosteal surface was only partly supported. At 3, 9, and 12 months, increases to overall density and trabecular density were

observed with HRpQCT, and were dependent on loading dose. However, contrary to our expectation, the inner trabecular density (Tb.BMDinn) rather than more peripheral regions appeared to be primarily affected. During aging, trabecular structure is first lost from this region, and later from more peripheral regions[37], thus maximizing moment of inertia for a given quantity of bone. We even observed age-associated declines in Tb.BMDinn within a large subset of the relatively narrow range of young healthy subjects measured here [38]. It is possible that in our cohort of young, healthy women, trabecular microstructure in the more peripheral regions was already at its physiologic maximum, limiting the degree to which it might be improved. However, even in this group, we observed Tb.BMDinn was lower than Tb.BMDmeta (Table 3), suggesting that there was greater capacity to improve the inner region with anabolic physical activity.

We observed significant positive effects of loading on Tt.BMD, Tb.BMDinn, and Ct.BMD after three months. Interestingly, all subjects were assigned the same loading magnitude (200 N) during this ramp-up period, rather than a group-specific strain. Compliance was also the best during the first three months. Therefore, it is not surprising that both low and high magnitude groups had increases in to these variables, since they both received the same stimulus. Overall, this supports the notion that loads must be novel to elicit an osteogenic response [18]. The improved response in the low magnitude group, who completed more loading bouts than other groups, also suggests that consistency of exercise is as important as strain magnitude and rate.

We observed significant increases to bone mass in the strain rate experiment; however, both low and high strain rate groups demonstrated positive results and the regression coefficients were similar between groups. Surprisingly, in Experiment 1 (strain magnitude) only the low strain magnitude group showed even slight increases in ultradistal iBMC after 12 months, with no observable changes in the high strain magnitude group. In fact, despite being given different target strains and strain rates, the different loading groups did not achieve the expected range of rates and magnitudes (Table 1). This, combined with varying subject compliance may partly explain these counterintuitive results. The analysis by tertile change in ultradistal iBMC suggests

an association between our dose measure of Strain_MagRate and changes to this measure. Subjects in the highest tertile also had higher baseline BMC, suggesting that perhaps these individuals simply had a greater physiologic capacity to respond to osteogenic stimuli. We did not observe any other obvious factors related to the change (e.g. vitamin D status) that might explain this, although our measurements did not include biomarkers related to bone metabolism. The degree to which strain magnitude can be manipulated is limited due to risk of secondary injury, although greater magnitudes are possible in the lower extremities. With vibration and other external assistance, it is possible to manipulate strain rate over a much wider range than strain magnitude.

In contrast to small animal *in vivo* loading models, which use a materials testing machine to generate a predictable and repeatable waveform, voluntarily applied forces are variable in terms of frequency content, even when the peak magnitude is guided through visual feedback, as in our study. While many measures of bone loading dose have been proposed in the literature, we found it impractical to implement any of them exactly as described by the authors. In addition to voluntarily produced loading signals being inconsistent, mechanical strain is non-uniform within a bone, both temporally and spatially; thus, no single strain value completely describes the strain occurring within a bone. Furthermore, it is not practical to place strain gages on most bones, and even when such measures are obtained (e.g. reference 39), they only represent a small fraction of the bone surface. Here, we examined several candidate versions of loading dose, based on recorded load cell signals and subject-specific FE models. Each version included a combination of strain magnitude, frequency, and number of loading bouts. As a first attempt, we chose to examine the actual strain produced within the analysis region in question (corresponding with the QCT or HRpQCT analysis region for those respective variables) and the total number of bouts achieved up to the timepoint in question. While we found significant associations between our measures of loading dose and changes to bone in our subjects, we found that at best, dose explained 17% of the variance in the change. It is possible that other formulations of loading dose that include local strain rate, strain gradient, or other measures, may be more relevant.

The magnitude and nature of the changes we observed are similar to an earlier, 6-month study using a similar loading protocol [26]. In that set of 19 young women, control subjects lost 1.7±1.1% ultradistal iBMC, while those in the loading group had no change in iBMC, but significant increases in trabecular BMC (1.3±2.8%). Here, we found a similar decrease in the control group iBMC (-1.3±2.7%), and increases to Tb.BMDinn that were associated with loading dose. The present cohort differed from the previous study in several ways. First, present subjects were generally older (28 vs. 22 years old) and many had a history of pregnancy or lactation (although not within the two years preceding enrollment). The present group were assigned loading magnitudes based on strain within the ultradistal radius at the instant of peak force production. However, due to limits on the force that subjects were able to safely produce voluntarily, subjects fell short of their target strains. Thus, while high strain magnitudes may have, in theory, elicited a greater osteogenic response, they were impractical to implement. Similarly, subjects in the low and high strain rate groups were given instruction sets designed to elicit significantly different strain rates. While the rates were significantly different between groups, (low: 675 με/s, high: 1394 με/s) the sample did not vary as widely as anticipated. And, both low and high strain rate groups experienced similar increases in bone. Distal radius compressive loading is a relatively constrained activity, and the ability to manipulate the strain signal was limited.

Our results suggest that, while compressive loading in general is osteogenic, it is not necessary to generate extremely high strain magnitudes or rates to elicit a positive response in the upper extremity. Our data show that gains in BMC are associated with moderate strain rates and magnitudes. Furthermore, these gains were achieved in a reasonable amount of time (100 loading cycles/bout, and an average of 131 loading bouts over a 12-month period for the highest tertile group). This is reassuring, since high loading rates have been linked to increased risk of stress fracture [40]. Although we did not systematically test the effect of loading cycles/bout, we based our target of 100 on (1) feasibility and time to complete the intervention, about three minutes, and (2) theoretical calculations of bone adaptation [36; 41] that suggested a diminished

osteogenic response with additional cycles. It is possible that the number of repetitive loading cycles, more than the strain signals from individual loading cycles themselves, is what tips the balance of a strain signal being positive/osteogenic to negative/increasing risk of injury.

This study had several important limitations. Only 60 of the 102 original subjects completed all 12 months of the study, and it is possible that our results are biased towards those who did not drop out. However, the demographics and baseline data of individuals who dropped out were not significantly different from those who completed the study. Due to the lower number of completers, our data were not powered enough to detect trabecular microstructural changes. However, these contributed collectively to the overall iBMC and Tb.BMD changes we observed. The magnitude of the increases to iBMC due to the loading interventions, 1.2% across all subjects, while modest, is not dissimilar to other treatment effects considered clinically relevant. And, subjects participating in Experiment 2 had much larger increases (2.9 and 3.6%). For comparison, a 3.3% increase in trochanter integral BMD over 36 months was observed in postmenopausal women given zolendronic acid [42], and it has been estimated that each 1% increase in peak bone mass imparts over 1 year of osteoporosis-free life in the future[43]. While the present study examined the effects of strain magnitude and rate on bone adaptation, an underlying assumption is that the bone of each individual is already well adapted for her habitual activities; our analysis only considered the novel/added stimulus. Although we collected physical activity data as part of this study, they were beyond the scope of the present analysis, but may potentially explain some of the variability in response to our intervention. Our results may not be generalizable to other populations, including postmenopausal women, those with low vitamin D, men, or specific clinical populations. Finally, more research is needed to determine the specific strain requirements to elicit clinically relevant changes to lower extremity bone, given the high habitual loading stimulus in these anatomic sites.

Although other clinical trials have investigated the efficacy of various types of exercise to for improving bone mass, this study is the first to systematically investigate the effect of mechanical strain rate and magnitude on bone adaptation in humans. The data presented here fill

a critical translational gap, linking *in vivo* animal models to clinical trials, and may be useful for informing the design of future clinical interventions for bone health. In particular, our data show that in healthy adult women, the distal radius is capable of modest adaptation in response to mechanical strain, and that the adaptation is associated with measures of loading dose that include strain magnitude, rate, and number of loading bouts.

In conclusion, we conducted a randomized prospective experiment to systematically investigate the effect of mechanical strain rate and magnitude on bone adaptation, using an *in vivo* upper extremity loading model in healthy adult women. We found that compressive loading in general was osteogenic, with high and low strain rate groups having similar significant increases to bone mass. We observed that subjects who gained the most bone had, on average, completed 130 compressive loading bouts, generating an average energy-equivalent strain of 550 με at 1805 με/s within the distal radius, over a period of 12 months. Individuals with the greatest gains to bone mass were similar in demographics to those with the lowest gains to bone mass. Those with the greatest gains had the highest Strain_MagRate loading dose. We conclude that signals related to strain magnitude, strain rate, and number of loading bouts collectively contribute to bone adaptation in healthy adult women.

Acknowledgements

This research was fully supported by NIAMS of the National Institutes of Health under award number R01AR063691.The content is solely the responsibility of the authors and does not necessarily represent the official views of the National Institutes of Health. We thank Sabahat Ahmed for her organization and dedication as research coordinator.

Author Contributions

Study conceived by KLT and designed by KLT with assistance from TJS. Data collection by MEM, KLT, JEJ, and TAB. Data analysis and interpretation: MEM, KLT, JEJ, TAB, ZW, TJS. Manuscript writing: KLT and MEM. Manuscript approval: MEM, KLT, JEJ, TAB, ZW, TJS.

References Cited

1. Howe TE, Shea B, Dawson LJ, et al. 2011. Exercise for preventing and treating osteoporosis in postmenopausal women. Cochrane database of systematic reviews (Online) (7):CD000333.
2. Weidauer L, Minett M, Negus C, et al. 2014. Odd-impact loading results in increased cortical area and moments of inertia in collegiate athletes. Eur J Appl Physiol 114:1429-1438.
3. Kontulainen SA, Kannus PA, Pasanen ME, et al. 2002. Does previous participation in high-impact training result in residual bone gain in growing girls? One year follow-up of a 9-month jumping intervention. Int J Sports Med 23:575-581.
4. Bailey CA, Brooke-Wavell K. 2010. Optimum frequency of exercise for bone health: randomised controlled trial of a high-impact unilateral intervention. Bone 46:1043-1049.
5. Korpelainen R, Keinanen-Kiukaanniemi S, Heikkinen J, et al. 2006. Effect of impact exercise on bone mineral density in elderly women with low BMD: a population-based randomized controlled 30-month intervention. Osteoporos Int 17:109-118.
6. LaMothe JM, Hamilton NH, Zernicke RF. 2005. Strain rate influences periosteal adaptation in mature bone. Med Eng Phys 27:277-284.
7. Mosley JR, Lanyon LE. 1998. Strain rate as a controlling influence on adaptive modeling in response to dynamic loading of the ulna in growing male rats. Bone 23:313-318.
8. O'Connor JA, Lanyon LE, MacFie H. 1982. The influence of strain rate on adaptive bone remodelling. Journal of Biomechanics 15:767-781.
9. Mosley JR, March BM, Lynch J, et al. 1997. Strain magnitude related changes in whole bone architecture in growing rats. Bone 20:191-198.
10. Rubin CT, Lanyon LE. 1985. Regulation of bone mass by mechanical strain magnitude. Calcified tissue international 37:411-417.

11. Donahue SW, Donahue HJ, Jacobs CR. 2003. Osteoblastic cells have refractory periods for fluid-flow-induced intracellular calcium oscillations for short bouts of flow and display multiple low-magnitude oscillations during long-term flow. J Biomech 36:35-43.
12. Steck R, Niederer P, Knothe Tate ML. 2000. A finite difference model of load-induced fluid displacements within bone under mechanical loading. Med Eng Phys 22:117-125.
13. Kowalchuk RM, Pollack SR. 1993. Stress-generated potentials in bone: effects of bone fluid composition and kinetics. J Orthop Res 11:874-883.
14. Hazenberg JG, Freeley M, Foran E, et al. 2006. Microdamage: a cell transducing mechanism based on ruptured osteocyte processes. J Biomech 39:2096-2103.
15. Burr DB, Martin RB, Schaffler MB, et al. 1985. Bone remodeling in response to in vivo fatigue microdamage. Journal of Biomechanics 18:189-200.
16. Muir P, Sample SJ, Barrett JG, et al. 2007. Effect of fatigue loading and associated matrix microdamage on bone blood flow and interstitial fluid flow. Bone 40:948-956.
17. Nguyen AM, Jacobs CR. 2013. Emerging role of primary cilia as mechanosensors in osteocytes. Bone 54:196-204.
18. Turner CH. 1998. Three rules for bone adaptation to mechanical stimuli. Bone 23:399-407.
19. Dolan SH, Williams DP, Ainsworth BE, et al. 2006. Development and reproducibility of the bone loading history questionnaire. Medicine and science in sports and exercise 38:1121-1131.
20. Weeks BK, Beck BR. 2008. The BPAQ: a bone-specific physical activity assessment instrument. Osteoporosis international 19:1567-1577.
21. Ahola R, Korpelainen R, Vainionpaa A, et al. 2010. Daily impact score in long-term acceleration measurements of exercise. Journal of Biomechanics 43:1960-1964.
22. Turner CH, Robling AG. 2003. Designing exercise regimens to increase bone strength. Exerc Sport Sci Rev 31:45-50.

23. Bhatia VA, Edwards WB, Troy KL. 2014. Predicting surface strains at the human distal radius during an in vivo loading task--finite element model validation and application. Journal of Biomechanics 47:2759-2765.

24. Gray HA, Taddei F, Zavatsky AB, et al. 2008. Experimental validation of a finite element model of a human cadaveric tibia. J Biomech Eng 130:031016.

25. Taddei F, Schileo E, Helgason B, et al. 2007. The material mapping strategy influences the accuracy of CT-based finite element models of bones: an evaluation against experimental measurements. Med Eng Phys 29:973-979.

26. Troy KL, Edwards WB, Bhatia VA, et al. 2013. In vivo loading model to examine bone adaptation in humans: a pilot study. Journal of orthopaedic research 31:1406-1413.

27. Bhatia VA, Edwards WB, Johnson JE, et al. 2015. Short-term bone formation is greatest within high strain regions of the human distal radius: a prospective pilot study. Journal of Biomechanical Engineering 137:10.1115/1111.4028847.

28. Baxter-Jones AD, Kontulainen SA, Faulkner RA, et al. 2008. A longitudinal study of the relationship of physical activity to bone mineral accrual from adolescence to young adulthood. Bone 43:1101-1107.

29. Henry YM, Fatayerji D, Eastell R. 2004. Attainment of peak bone mass at the lumbar spine, femoral neck and radius in men and women: relative contributions of bone size and volumetric bone mineral density. Osteoporosis international 15:263-273.

30. Oldfield RC. 1971. The assessment and analysis of handedness: the Edinburgh inventory. Neuropsychologia 9:97-113.

31. Buie HR, Campbell GM, Klinck RJ, et al. 2007. Automatic segmentation of cortical and trabecular compartments based on a dual threshold technique for in vivo micro-CT bone analysis. Bone 41:505-515.

32. Burghardt AJ, Buie HR, Laib A, et al. 2010. Reproducibility of direct quantitative measures of cortical bone microarchitecture of the distal radius and tibia by HR-pQCT. Bone 47:519-528.

33. Burghardt AJ, Kazakia GJ, Link TM, et al. 2009. Automated simulation of areal bone mineral density assessment in the distal radius from high-resolution peripheral quantitative computed tomography. Osteoporos Int 20:2017-2024.

34. Edwards WB, Schnitzer TJ, Troy KL. 2014. Bone mineral and stiffness loss at the distal femur and proximal tibia in acute spinal cord injury. Osteoporosis int 25:1005-1015.

35. Edwards WB, Troy KL. 2012. Finite element prediction of surface strain and fracture strength at the distal radius. Med Eng Phys 34:290-298.

36. Mikic B, Carter DR. 1995. Bone strain gage data and theoretical models of functional adaptation. J Biomech 28:465-469.

37. Sode M, Burghardt AJ, Kazakia GJ, et al. 2010. Regional variations of gender-specific and age-related differences in trabecular bone structure of the distal radius and tibia. Bone 46:1652-1660.

38. Mancuso M, Johnson J, Ahmed S, et al. 2018. Distal radius microstructure and finite element bone strain are related to site-specific mechanical loading and areal bone mineral density in premenopausal women. Bone Reports 8:187-194.

39. Milgrom C, Burr DB, Finestone AS, et al. 2015. Understanding the etiology of the posteromedial tibial stress fracture. Bone 78:11-14.

40. Zadpoor AA, Nikooyan AA. 2011. The relationship between lower-extremity stress fractures and the ground reaction force: a systematic review. Clin Biomech 26:23-28.

41. Bhatia VA, Edwards WB, Troy KL. 2013. Predicting bone adaptation at the human distal radius using cadaveric specimens and the Daily Strain Stimulus theory. Proceedings of the 59th Annual Meeting of the Orthopaedic Research Society San Antonio, TX.

42. Eastell R, Lang T, Boonen S, et al. 2010. Effect of once-yearly zoledronic acid on the spine and hip as measured by quantitative computed tomography: results of the HORIZON Pivotal Fracture Trial. Osteoporosis international 21:1277-1285.

43. Hernandez CJ, Beaupre GS, Carter DR. 2003. A theoretical analysis of the relative influences of peak BMD, age-related bone loss and menopause on the development of osteoporosis. Osteoporos Int 14:843-847.

List of Figures and Tables

Figure 1. A. Summary of the data collection timeline for participants assigned to exercise groups; **B.** Loading device used to manipulate applied force magnitude via feedback lights (green set to target force minus 10 N, red to target force plus 10 N). Loading frequency was controlled using pre-recorded auditory cues. The force vs. time curve shows a representative load cell signal (black) versus ideal assigned loading stimulus (gray), with dashed lines indicating the forces at which feedback is given; **C.** Linear FE model used to estimate energy equivalent strain in the transverse section matching the imaged site. The force-strain relationship was used to assign each subject a target force and calculate the resulting strain from load cell recordings.

Figure 2. Consort chart describing participant flow.

Figure 3. Effect of Strain_MagRate on 12-month changes to bone: **A.** ultradistal iBMC, **B.** ultradistal CSA, and **C.** Tb.vBMDinn.

Figure 4. A. Ct.vBMD, **B.** Tb.vBMDinn, and **C.** Tt.BMD,versus time, per group. Significant group changes at specific timepoints are labeled with *. Error bars represent standard error.

Table 1. Mean (SD) baseline subject characteristics (a), and loading intervention by group (b). Strain magnitudes were assigned based on the maximum energy-equivalent strain within the ultradistal region, as calculated by FE model. However, for loading dose calculations, the achieved mean energy-equivalent strain was used, since it better represents the strain experienced within the region.

Table 2. Mean (SD) baseline of the pooled data, and percent change at 12 months in QCT variables, by group.

Table 3. Mean (SD) of baseline and percent changes of HRpQCT measures during each visit (V1 at baseline through V5 at 12 months), by group.

Table 4. Regression coefficients for QCT, by group and by loading dose. Low1 and High1 indicate low and high strain magnitude groups from Experiment 1. Low2 and High2 indicate low and high strain rate groups from Experiment 2.

Table 5. Mean (SD) grouped by change in ultradistal iBMC tertile. P-values indicate significant between-group differences. Symbols indicate significant Bonferroni-adjusted post hoc comparisons between specific tertiles.

Figure 1

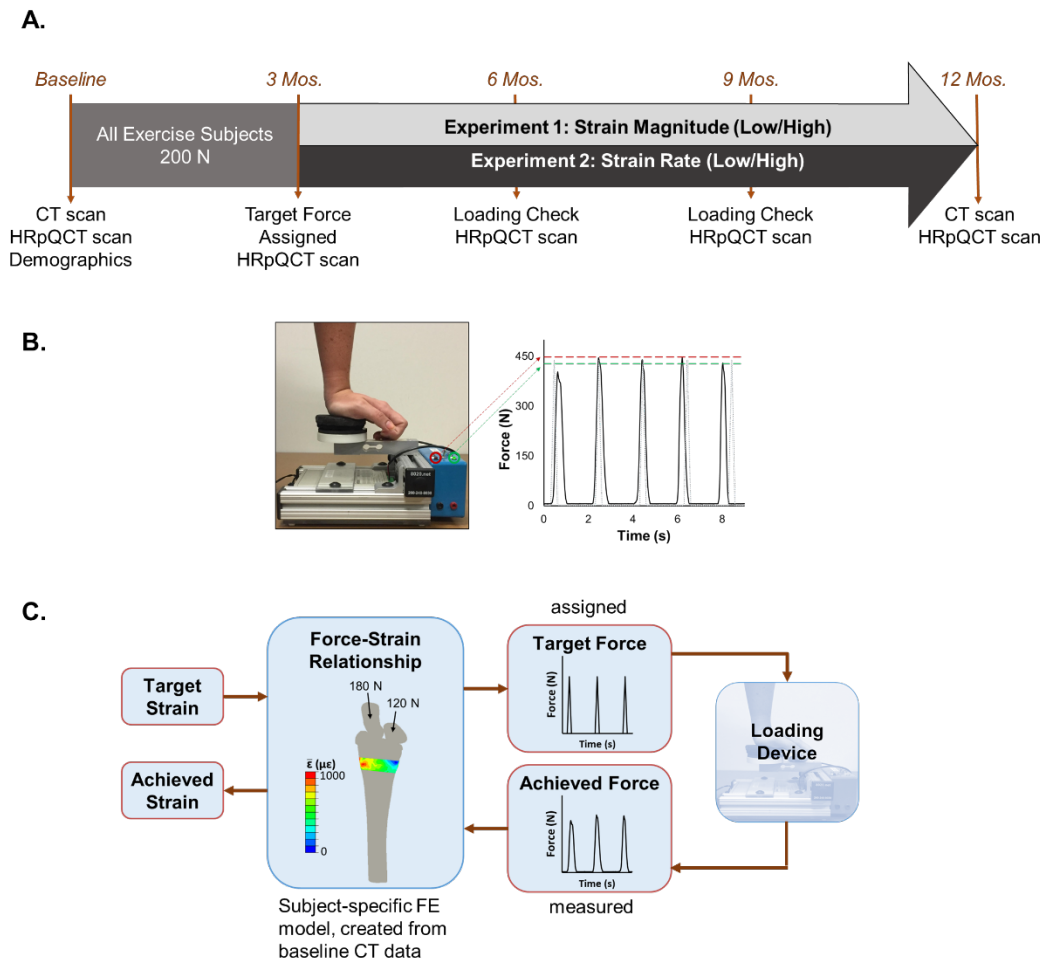

Figure 2

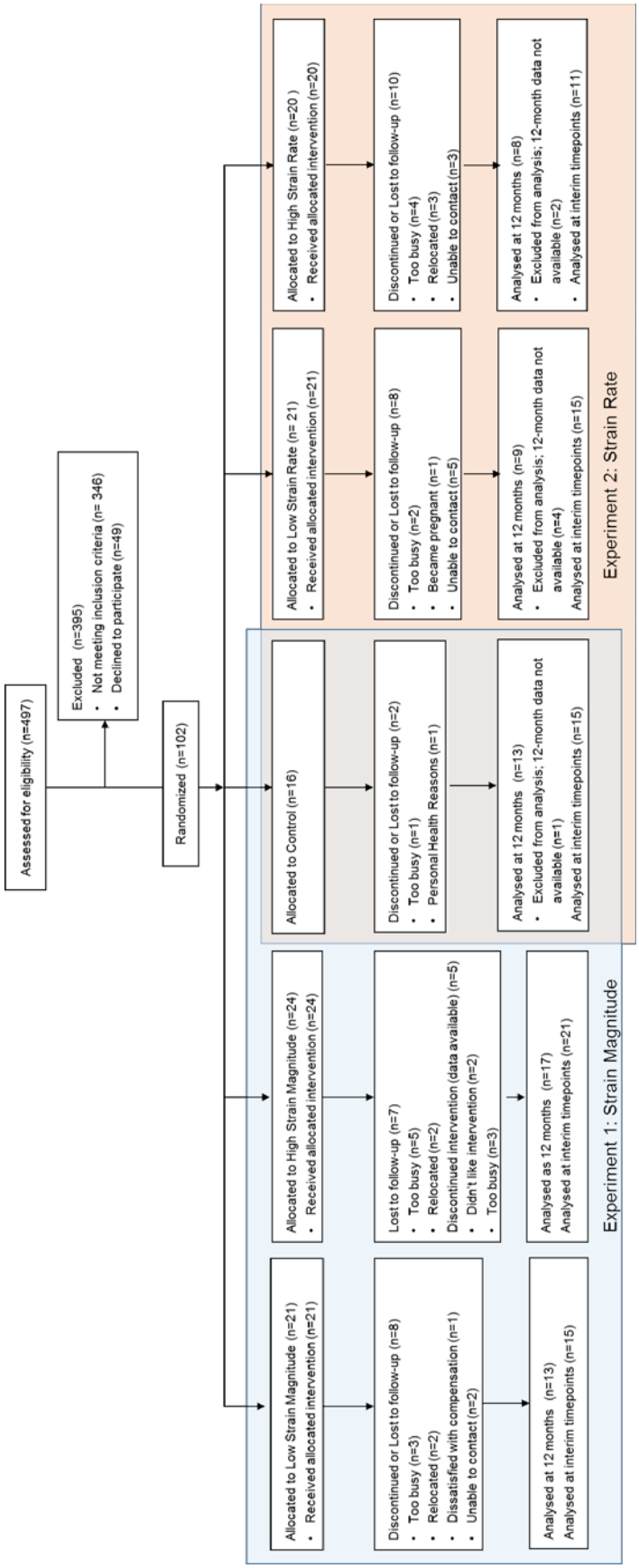
Assessed for eligibility (n=497)
Excluded (n=395)
• Not meeting inclusion criteria (n= 346)
• Declined to participate (n=49)
Randomized (n=102)
Allocated to Low Strain Rate (n=21)
• Received allocated intervention (n=21)
Discontinued or Lost to follow-up (n=8)
• Too busy (n=3)
• Relocated (n=2)
• Dissatisfied with compensation (n=1)
• Unable to contact (n=2)
Analysed at 12 months (n=13)
Analysed at interim timepoints (n=15)
Allocated to High Strain Magnitude (n=24)
• Received allocated intervention (n=24)
Lost to follow-up (n=7)
• Too busy (n=5)
• Relocated (n=2)
Discontinued intervention (data available) (n=5)
• Didn't like intervention (n=2)
• Too busy (n=3)
Analysed as 12 months (n=17)
Analysed at interim timepoints (n=21)
Experiment 1: Strain Magnitude
Allocated to Control (n=16)
Discontinued or Lost to follow-up (n=2)
• Too busy (n=1)
• Personal Health Reasons (n=1)
Analysed at 12 months (n=13)
• Excluded from analysis; 12-month data not available (n=1)
Analysed at interim timepoints (n=15)
Allocated to Low Strain Rate (n= 21)
• Received allocated intervention (n=21)
Discontinued or Lost to follow-up (n=8)
• Too busy (n=2)
• Became pregnant (n=1)
• Unable to contact (n=5)
Analysed at 12 months (n=9)
• Excluded from analysis; 12-month data not available (n=4)
Analysed at interim timepoints (n=15)
Allocated to High Strain Rate (n=20)
• Received allocated intervention (n=20)
Discontinued or Lost to follow-up (n=10)
• Too busy (n=4)
• Relocated (n=3)
• Unable to contact (n=3)
Analysed at 12 months (n=8)
• Excluded from analysis; 12-month data not available (n=2)
• Analysed at interim timepoints (n=11)
Experiment 2: Strain Rate

Figure 3 **A.**

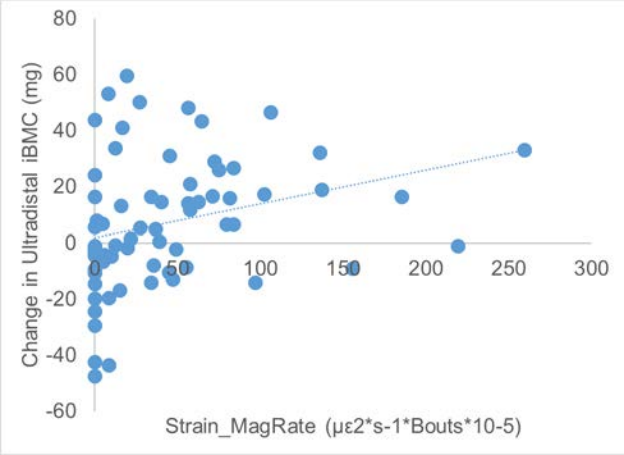
Change in Ultradistal iBMC (mg)
80
60
40
20
0
-20
-40
-60
0
50
100
150
200
250
300
Strain_MagRate (με2*s-1*Bouts*10-5)

B.

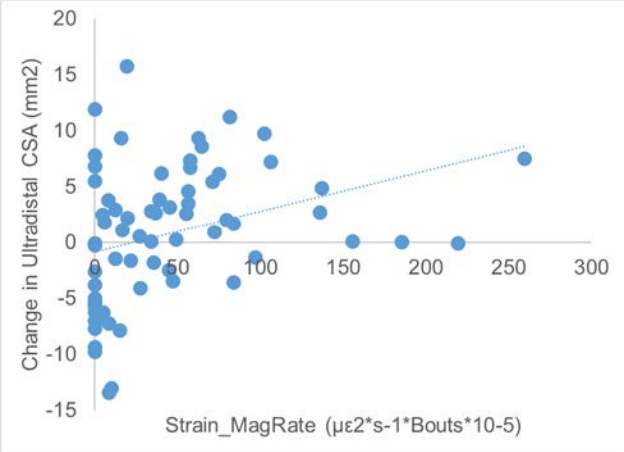
Change in Ultradistal CSA (mm2)
20
15
10
5
0
-5
-10
-15
0
50
100
150
200
250
300
Strain_MagRate (με2*s-1*Bouts*10-5)

C.

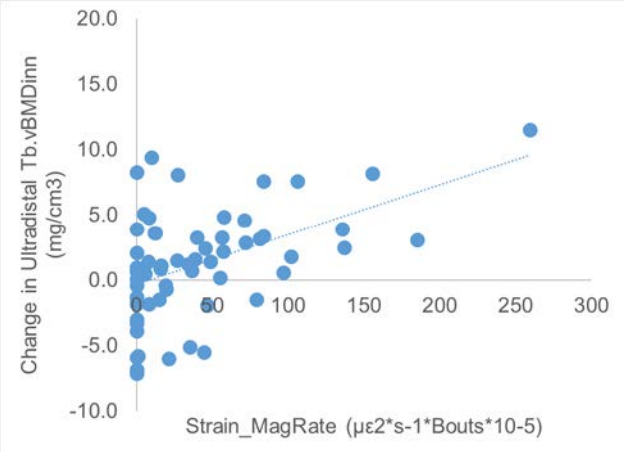
Change in Ultradistal Tb.vBMDinn (mg/cm3)
20.0
15.0
10.0
5.0
0.0
-5.0
-10.0
0
50
100
150
200
250
300
Strain_MagRate (με2*s-1*Bouts*10-5)

Figure 4. A.

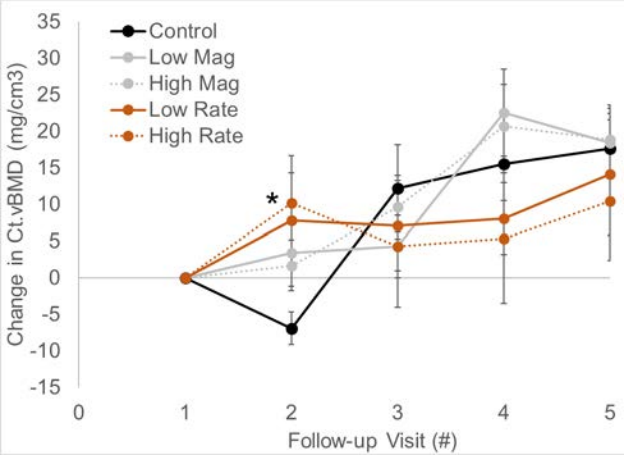
Control
Low Mag
High Mag
Low Rate
High Rate
Change in Ct.vBMD (mg/cm3)
Follow-up Visit (#)

B.

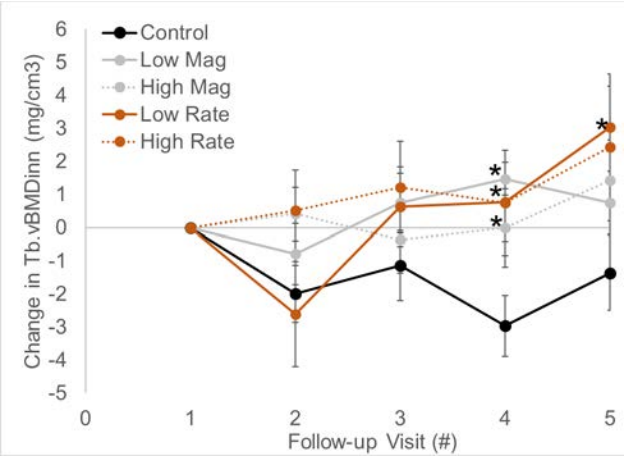
Control
Low Mag
High Mag
Low Rate
High Rate
Change in Tb.vBMDinn (mg/cm3)
Follow-up Visit (#)

C.

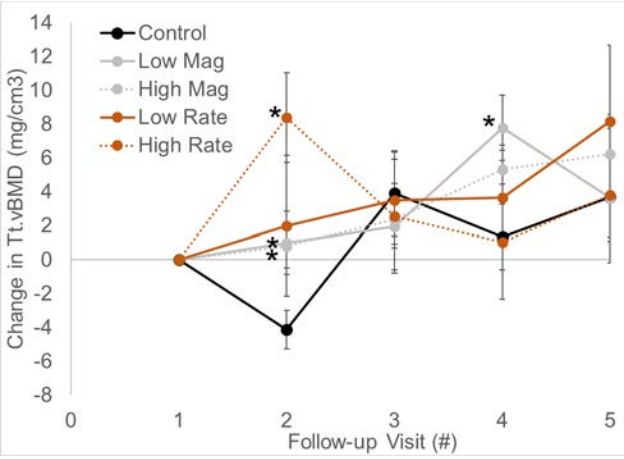
Control
Low Mag
High Mag
Low Rate
High Rate
Change in Tt.vBMD (mg/cm3)
Follow-up Visit (#)

Table 1a.

Subject Characteristics	n=102	
Demographics		
Age (years)	28.4	(5.6)
Height (cm)	164.3	(8.4)
Body Mass (kg)	64.5	(8.7)
Serum Vitamin D (ng/mL)	31.7	(9.5)
Total Forearm aBMD (g/cm^2)	0.57	(0.04)
Total Forearm T-score	-0.09	(0.70)
Ethnicity n (%)		
Hispanic or Latino	12	(12)
Non-Hispanic	89	(87)
Not Reported	1	(1)
Race n (%)		
African American	1	(1)
Caucasian	76	(75)
Asian	12	(12)
Pacific Islander	1	(1)
More Than One Race	7	(7)
Not Reported	5	(5)

Table 1b.

Treatment Group	Low Magnitude		High Magnitude		Low Rate		High Rate	
	n=21		n=24		n=21		n=20	
Prescribed Loading								
Number of Sessions	208		208		208		208	
Max Ultradistal Strain Magnitude (με)	1800		3600		3600		3600	
Mean Ultradistal Strain Magnitude (με)	490	(103)	748	(143)	632	(138)	641	(157)
Strain Rate (based on Mean Strain) (με/s)	1485	(312)	2267	(434)	790	(173)	6410	(1570)
Achieved Loading								
Number of Sessions	121	(101)	80	(78)	64	(67)	63	(90)
Mean Ultradistal Strain Magnitude (με)	344	(200)	369	(203)	352	(281)	450	(241)
Strain Rate (based on Mean Strain) (με/s)	921	(650)	1259	(1149)	675	(605)	1394	(1204)
StrainStim ($\mu\varepsilon*s^{-1}*Files*10^{-7}$)	141	(193)	118	(240)	35	(73)	53	(83)
Strain_MagRate ($\mu\varepsilon^2*s^{-1}*Files*10^{-5}$)	319	(353)	428	(651)	198	(254)	368	(466)
Strain_Mag ($\mu\varepsilon*Files*10^{-2}$)	493	(435)	463	(518)	325	(347)	383	(442)
Strain_Rate ($\mu\varepsilon*s^{-1}*Files*10^{-3}$)	130	(135)	141	(186)	68	(90)	136	(181)

Table 2

	Total (n=60)		Control (n=13)		Low Magnitude (n=13)		High Magnitude (n=17)		Low Rate (n=9)		High Rate (n=8)	
	Baseline		**% Change**		**% Change**		**% Change**		**% Change**		**% Change**	
Ultradistal												
iBV (cm^3)	3.80	(0.36)	-1.17	(2.51)	**0.75**	**(2.14)**	-0.01	(2.23)	-0.49	(2.25)	1.03	(2.48)
iBMC (g)	0.91	(0.14)	-1.31	(2.68)	**0.46**	**(1.52)**	-0.33	(2.03)	**2.90**	**(2.02)**	**3.61**	**(2.33)**
iBMD (g/cm^3)	0.24	(0.03)	-0.59	(2.08)	-0.23	(0.96)	-0.33	(1.19)	**3.19**	**(0.80)**	**2.74**	**(1.47)**
ecBV (cm^3)	1.98	(0.13)	-0.41	(1.49)	**0.89**	**(1.39)**	0.34	(1.58)	-0.08	(1.37)	0.45	(1.44)
ecBMC (g)	0.63	(0.17)	-0.19	(4.87)	0.12	(2.46)	-0.10	(2.62)	**5.38**	**(3.02)**	3.98	(3.07)
ecBMD (g/cm^3)	0.32	(0.07)	6.11	(133.32)	-33.89	(155.63)	13.26	(201.61)	62.77	(91.37)	60.41	(62.78)
Total												
iBV (cm^3)	12.83	(1.48)	-0.06	(0.47)	-0.25	(0.52)	-0.13	(0.45)	0.29	(0.67)	**0.47**	**(0.41)**
iBMC (g)	5.08	(0.58)	-0.23	(1.20)	-0.45	(0.80)	-0.19	(0.78)	**2.09**	**(0.68)**	**1.81**	**(0.84)**
iBMD (g/cm^3)	0.40	(0.03)	-0.17	(1.14)	-0.19	(0.58)	-0.06	(0.78)	**1.80**	**(0.46)**	**1.33**	**(0.84)**
ecBV (cm^3)	8.19	(0.68)	0.17	(0.71)	-0.07	(0.57)	0.18	(0.44)	0.54	(0.52)	0.25	(0.65)
ecBMC (g)	4.09	(0.52)	0.15	(1.78)	-0.26	(1.11)	0.00	(1.01)	**2.28**	**(1.20)**	1.57	(1.18)
ecBMD (g/cm^3)	0.50	(0.05)	-0.02	(1.28)	-0.20	(0.76)	-0.18	(0.98)	**1.73**	**(0.79)**	**1.32**	**(0.67)**
Ultradistal Strength												
CSA (cm^2)	4.11	(0.39)	-0.67	(1.67)	**0.65**	**(1.45)**	0.00	(1.48)	-0.25	(1.40)	0.83	(1.75)
CSI (g^2/cm^4)	0.24	(0.07)	-1.81	(4.40)	0.18	(1.96)	-0.65	(2.85)	**6.23**	**(2.71)**	**6.44**	**(3.41)**
BSI (cm^3)	0.12	(0.03)	-0.59	(4.31)	0.32	(1.90)	-0.29	(2.30)	**4.85**	**(2.47)**	**4.66**	**(2.57)**
I_{min} (g x mm^2)	1.80	(0.38)	1.77	(9.13)	9.56	(36.72)	5.27	(30.51)	-0.74	(3.17)	0.36	(4.97)
I_{max} (g x mm^2)	4.80	(0.94)	1.72	(7.15)	10.78	(37.24)	2.22	(26.67)	0.16	(2.41)	1.86	(3.00)
J_o (g x mm^2)	6.59	(1.30)	1.70	(7.33)	10.33	(36.84)	2.99	(27.51)	-0.08	(2.61)	1.43	(3.19)

Bold indicates significant regression coefficient representing contrast with control group for raw change.

Table 3

		Baseline		%ΔV2		%ΔV3		%ΔV4		%ΔV5	
Control	Tt.BMD (g/cm^3)	292.46	(45.29)	-1.35	(1.16)	1.29	(2.90)	0.36	(2.25)	1.52	(3.67)
	Tb.BMD (g/cm^3)	168.94	(36.08)	-1.21	(1.75)	-0.54	(2.14)	-1.78	(2.30)	-0.15	(3.61)
	Tb.BMD$_{Meta}$ (g/cm^3)	226.58	(37.12)	-0.71	(1.19)	-0.14	(2.09)	-0.83	(1.88)	0.76	(3.75)
	Tb.BMD$_{Inn}$ (g/cm^3)	129.13	(37.03)	-2.01	(2.87)	-1.04	(2.49)	-2.96	(3.08)	-1.43	(3.91)
	Ct.BMD (g/cm^3)	851.54	(42.73)	-0.79	(0.80)	1.46	(2.65)	1.83	(2.03)	2.14	(1.69)
	Tb.N (mm^{-1})	2.09	(0.27)	-1.40	(5.81)	0.55	(12.01)	2.20	(7.55)	4.70	(7.90)
	Tb.Th (mm)	0.07	(0.01)	0.40	(4.94)	0.19	(11.92)	-3.35	(7.55)	-4.18	(8.63)
	Ct.Th (mm)	0.72	(0.09)	-0.42	(2.46)	0.47	(2.46)	-0.33	(2.94)	0.49	(3.38)
	Ct.Po (%)	0.01	(0.01)	-3.61	(15.33)	3.29	(18.50)	10.98	(21.33)	12.47	(18.81)
Low Magnitude	Tt.BMD (g/cm^3)	305.66	(56.40)	**0.39**	**(1.98)**	0.70	(3.06)	**2.59**	**(2.28)**	1.23	(2.71)
	Tb.BMD (g/cm^3)	157.28	(28.74)	-0.23	(1.73)	0.62	(2.41)	**1.06**	**(1.46)**	-0.04	(1.96)
	Tb.BMD$_{Meta}$ (g/cm^3)	220.84	(28.96)	-0.08	(1.74)	0.55	(2.01)	**0.91**	**(1.94)**	-0.37	(1.57)
	Tb.BMD$_{Inn}$ (g/cm^3)	113.34	(30.02)	-0.42	(2.55)	0.71	(3.36)	**1.35**	**(1.55)**	0.43	(3.13)
	Ct.BMD (g/cm^3)	883.92	(46.19)	0.38	(1.57)	0.50	(1.77)	2.58	(2.28)	2.12	(1.84)
	Tb.N (mm^{-1})	1.95	(0.24)	-2.56	(6.43)	-1.86	(8.31)	0.57	(8.51)	-1.07	(10.21)
	Tb.Th (mm)	0.07	(0.01)	2.74	(6.21)	2.99	(7.36)	0.99	(7.34)	1.90	(10.31)
	Ct.Th (mm)	0.81	(0.17)	0.23	(2.36)	-0.09	(4.64)	0.28	(2.05)	-0.98	(3.25)
	Ct.Po (%)	0.01	(0.00)	-7.19	(13.85)	11.33	(30.73)	7.59	(34.34)	9.83	(32.27)
High Magnitude	Tt.BMD (g/cm^3)	292.59	(55.28)	**0.29**	**(1.92)**	0.90	(1.94)	1.98	(1.84)	2.16	(3.07)
	Tb.BMD (g/cm^3)	162.39	(31.41)	0.20	(2.16)	-0.32	(2.30)	-0.23	(1.99)	0.72	(2.39)
	Tb.BMD$_{Meta}$ (g/cm^3)	220.08	(30.15)	0.05	(1.98)	-0.34	(1.71)	-0.25	(1.17)	0.47	(1.84)
	Tb.BMD$_{Inn}$ (g/cm^3)	122.55	(32.84)	0.43	(2.80)	-0.36	(3.52)	**-0.26**	**(3.30)**	0.95	(3.65)
	Ct.BMD (g/cm^3)	856.44	(45.47)	0.19	(1.74)	1.16	(1.94)	2.50	(2.35)	2.23	(2.08)
	Tb.N (mm^{-1})	2.00	(0.22)	-1.52	(6.33)	2.00	(6.78)	0.32	(11.14)	2.06	(9.07)
	Tb.Th (mm)	0.07	(0.01)	2.22	(7.40)	-1.90	(6.49)	0.53	(10.37)	-0.57	(8.25)
	Ct.Th (mm)	0.75	(0.16)	-0.94	(4.89)	0.11	(2.97)	-0.34	(6.12)	-0.16	(3.60)
	Ct.Po (%)	0.01	(0.01)	4.24	(24.66)	10.71	(28.76)	21.13	(70.73)	15.54	(28.43)
Low Rate	Tt.BMD (g/cm^3)	317.50	(54.62)	0.97	(4.23)	1.00	(3.43)	1.12	(3.10)	2.65	(4.46)
	Tb.BMD (g/cm^3)	165.05	(31.50)	-1.22	(3.12)	0.74	(2.00)	0.17	(1.88)	1.25	(2.55)
	Tb.BMD$_{Meta}$ (g/cm^3)	221.66	(28.83)	-0.92	(2.80)	0.57	(1.77)	-0.06	(1.45)	0.14	(2.17)
	Tb.BMD$_{Inn}$ (g/cm^3)	125.88	(34.33)	-1.62	(3.64)	0.88	(2.74)	**0.43**	**(3.09)**	**2.66**	**(3.77)**
	Ct.BMD (g/cm^3)	905.44	(54.81)	0.92	(2.29)	0.83	(2.34)	0.92	(1.97)	1.59	(2.77)
	Tb.N (mm^{-1})	2.06	(0.29)	-3.47	(6.46)	3.17	(11.74)	3.14	(10.78)	2.48	(9.64)
	Tb.Th (mm)	0.07	(0.01)	2.71	(7.25)	-1.18	(10.99)	-1.98	(10.40)	-0.30	(9.85)
	Ct.Th (mm)	0.80	(0.15)	1.43	(4.27)	0.88	(3.22)	0.70	(2.54)	1.64	(2.79)
	Ct.Po (%)	0.01	(0.01)	-5.04	(22.35)	4.25	(37.07)	7.33	(20.35)	8.66	(28.73)
High Rate	Tt.BMD (g/cm^3)	313.83	(42.68)	**2.78**	**(3.09)**	0.87	(3.73)	0.34	(3.03)	1.39	(3.39)
	Tb.BMD (g/cm^3)	156.46	(28.97)	-0.04	(1.82)	0.34	(2.05)	-0.56	(2.49)	1.00	(2.44)
	Tb.BMD$_{Meta}$ (g/cm^3)	215.45	(28.07)	-0.09	(1.29)	0.05	(1.64)	-1.01	(2.06)	0.34	(2.21)

	Tb.BMD$_{Inn}$ (g/cm^3)	115.66	(30.34)	-0.22	(3.65)	0.91	(3.73)	0.23	(3.63)	1.93	(3.76)
	Ct.BMD (g/cm^3)	913.44	(40.74)	**1.13**	**(2.28)**	0.52	(2.94)	0.64	(2.65)	1.17	(2.36)
	Tb.N (mm^{-1})	1.93	(0.24)	3.37	(9.27)	5.15	(10.97)	0.17	(9.69)	1.27	(11.10)
	Tb.Th (mm)	0.07	(0.01)	-2.66	(7.35)	-3.66	(9.25)	-0.09	(8.89)	0.66	(9.51)
	Ct.Th (mm)	0.83	(0.11)	**3.74**	**(3.64)**	0.47	(3.18)	-1.06	(2.61)	0.20	(3.75)
	Ct.Po (%)	0.01	(0.01)	-3.93	(23.04)	0.26	(21.38)	**-2.21**	**(27.96)**	7.66	(29.05)

Bold indicates significant regression coefficient representing contrast with control group for raw change.

Table 4

	Model Definition	**R^2**	**β_1**	**β_2**
UD iBMC (g)	β1*Low1+β2*High1+ε	0.101	**0.374**	0.221
	β1*Low2+β2*High2+ε	**0.465**	**0.604**	**0.634**
	β1*StrainStim+ε	0.016	0.128	
	β1*Strain_MagRate+ε	**0.082**	**0.286**	
	β1*Strain_Mag+ε	**0.083**	**0.289**	
	β1*Strain_Rate+ε	0.062	0.249	
UD iBMD (g/cm^3)	β1*Low1+β2*High1+ε	0.009	0.091	0.101
	β1*Low2+β2*High2+ε	**0.589**	**0.753**	**0.631**
	β1*StrainStim+ε	0.003	-0.057	
	β1*Strain_MagRate+ε	0.008	0.092	
	β1*Strain_Mag+ε	0.004	0.060	
	β1*Strain_Rate+ε	0.008	0.087	
Total iBMC (g)	β1*Low1+β2*High1+ε	0.019	-0.119	0.028
	β1*Low2+β2*High2+ε	**0.576**	**0.759**	**0.600**
	β1*StrainStim+ε	0.020	-0.143	
	β1*Strain_MagRate+ε	0.001	-0.032	
	β1*Strain_Mag+ε	0.004	-0.061	
	β1*Strain_Rate+ε	0.001	-0.031	
Total iBMD (g/cm^3)	β1*Low1+β2*High1+ε	0.005	-0.018	0.059
	β1*Low2+β2*High2+ε	**0.521**	**0.739**	**0.538**
	β1*StrainStim+ε	0.004	-0.067	
	β1*Strain_MagRate+ε	0.003	0.050	
	β1*Strain_Mag+ε	0.001	0.039	
	β1*Strain_Rate+ε	0.003	0.052	

Bold For R^2 indicates $p<0.05$ for F-test of overall model fit
Bold For β_1 or β_2 indicates $p<0.05$ for t-test of significance for coefficient

Table 5

	Highest Tertile	Middle Tertile	Lowest Tertile	P-value
Demographics				
Age (years)	26.9 (4.1)	29.3 (6.1)	29.1 (5.6)	0.294
Height (cm)	166 (7)	165 (6)	165 (7)	0.857
Body Mass (kg)	64.4 (9.1)	64.8 (8.2)	63.0 (7.3)	0.798
Serum Vitamin D (ng/mL)	30 (10)	31 (9)	34 (7)	0.377
Total Forearm aBMD (g/cm^2)	0.59 (0.03)	0.57 (0.04)	0.58 (0.04)	0.157
Group Membership (n; control/exercise)	2/18	3/17	8/12	-
Applied Loads				
Peak force (N)	297 (109)*	217 (136)	156 (140)	0.004
Loading rate (N/s)	857 (606)*	543 (537)	384 (423)	0.021
Number of Sessions	131 (91)	77 (77)	69 (85)	0.048
Peak Strain (με)	550 (221)*	449 (328)	313 (296)	0.037
Strain rate (με/s)	1805 (1489)	1166 (1016)	925 (1126)	0.073
StrainStim (με*s^{-1}*Files*10^{-7})	194 (267)	63.2 (100)	133 (232)	0.161
Strain_MagRate (με^2*s^{-1}*Files*10^{-5})	737 (673)*	352 (515)	257 (400)	0.016
Strain_Mag (με*Files*10^{-2})	786 (508)	501 (587)	371 (504)	0.05
Strain_Rate (με*s^{-1}*Files*10^{-3})	250 (232)	125 (161)	110 (149)	0.038
Bone QCT values				
Baseline ultradistal iBMC	0.987 (0.168)*	0.901 (0.129)	0.851 (0.117)	0.011
Visit 5 change (mg)	33 (14)*+	4 (6)*	-18 (13)+	<0.001
Visit 5 percent change (%)	3.6 (1.5)*+	0.5 (0.7)*	-2.1 (1.6)+	<0.001

* p<0.05 vs. lowest tertile +p<0.05 vs. middle tertile